

## Research on the Surface Defect Detection of Magnetic Sheet for Industrial Manufacture

Wenbo Zhang, RongweiDuan, YongxinFeng\* and Deyu Zhang

*School of Information Science and Engineering  
Shenyang Ligong University*

*No.6 Nanping Center Road, Hunnan New District, Shenyang 110159, P. R. China*

*\*Corresponding author: Fengyongxin@263.net*

### **Abstract**

*The research of defect detection technology of magnetic sheet surface has important significance for improvement of production efficiency and product quality in enterprise. A single threshold method is used for binary segmentation of magnetic sheet image in this paper, then the template localization algorithm is used for template position of magnetic sheet image after binary segmentation, the magnetic sheet image with different position should be transformed into a unified coordinate system for detecting, then least square method is used for fitting straight line and fillet edge, then the calculated values are compared with standard value to determine whether are knock edges. Further, the appropriate grayscale threshold is set by the pitting and scratches characteristics of magnetic sheet image, the magnetic sheet image should be segmented according to the determined threshold value, if the defect exists, the defect area or length will be calculated, then the result is compared with standard values to determine whether is pitting or scratches. The final tests of technology in this paper show that the detection rate of knock edge and the detection rate of pitting or scratches are both acceptable.*

**Keyword:** *Magnetic sheet, Machine vision, Surface defect detection, Least squares, Curve fitting, Gray threshold*

### **1. Summarize**

Magnetic sheet is a kind of material made of sintered NdFeB permanent magnet, which is widely used in areas such as electric motors, speaker motors and so on. In order to guarantee the product quality of magnetic sheet, it is needed to pass rigorous quality detection before the magnetic sheet becomes a product. The traditional product testing of magnetic sheet relies on manual detection, and there are great limitations in this way, which are mainly reflected on the following aspects: (1) human eyes have limited capacity in spatial distinguish. Some questions cannot be identified by human eyes, for example micro size and the lesser color aberration gray-level image or a defect existing in a complex background pattern, therefore it is very difficult to achieve complete detection of product defects; (2) Human eye's time resolution is limited, so it is difficult to monitor the whole process of product quality; (3) Manual detection will be affected by subjective awareness, which will lead to a great unreliability. The non-standard detection is harmful to product quality control and many unstable factors are able to be caused. And manual detection needs a huge amount of cost; the results of detection and defect shape are difficult to be recorded and to be saved, and manual detection leads to inconvenience of information management [1, 2].

In recent years, the technology of surface defect detection has been widely concerned in the field of magnetic sheet quality detection and the certain application has been obtained. However, because of wide scope of application of magnetic sheet, the magnetic sheet has various shapes, therefore, it is difficult to adopt a method to adapt to all types of

magnetic sheet surface defect detection, for this reason, a method that is fit for the square piece fillet detection of magnetic sheet has been proposed for industrial production in this paper, which has high detection accuracy and low missing rate.

## 2. Related Work

Image segmentation means that image is divided into sub-areas or objects, and image segmentation is the basis of defect detection. Image segmentation is divided into two categories based on discontinuity and similarity of the image gray [3, 4]. One is based on the discontinuity of image gray, such as segmentation of edge detection of image [5]; the other is based on the similarity of image gray, such as threshold processing, region growing and regional separation [6-8]. Zhang Yong and others put forward an improved method of graph theory threshold segmentation, which adequately considers the correlation between pixels. Li Sen and others put forward a thresholding segmentation method of improved regional division of the two-dimensional histogram, which is a new modified algorithm direct at the traditional OTSU's problems about low Segmentation accuracy or classification error and other problems. There are many other modified thresholding segmentation algorithms [9-12]. Image segmentation based on edge detection is an important algorithm of image segmentation, as the whole, it is divided into two categories: method of differential operator and method of surface fitting. Differential operator finds the image edge through a first or second order derivative calculation, and the primary detection operators include Roberts, Sobel, Prewitt, Kirsch, Laplacian, Log and so on [13]. Surface fitting uses flat or curved surface to gain on surface element of the gray image, then the gradient is used to replace its gradient of pixel in order to realize edge detection [14, 15]. Wang Junhui, Li Kerui, Liu Xiaoyang put forward a real-time edge detection system based on the modified Sobel algorithm, the algorithm is a new modified algorithm direct at the traditional Sobel operator detection method which has disadvantages like noise sensitivity and poor self-adaption. Zhang Jianjun, Luo Jing put forward a surface crack edge detection algorithm based on modified Sobel operator, which solves inaccuracy edge positioning of image and sensitive to noise [16]. In recent years, with the development of theory, many new image segmentation algorithms have emerged. Such as the partition method of mathematical morphology in [17], the watershed image division combined with Wavelet transform in [18], the split-horizon in [19], the modified immune genetic algorithm used for image segmentation in [20], and the partition method with fuzzy theory in [21]. Because of the uncertainty and complexity of image, the segmentation algorithm fit for all images has not appeared, and the appropriate segmentation algorithm should be designed according to the actual research object.

The feature extraction and description of image is for the sake of reducing the data dimension further, and the image information is converted into abstract features, then the information could provide help for high level understanding of image [22]. Image features can be divided into grayscale, texture, geometry, spectrum, projectors and other features [23], geometric features include area, centroid, circularity, Euler number and so on [24], grayscale features include grayscale average, grayscale variance, entropy and so on, texture [25]. For the detection of surface defects, it is needed to further identify and judge the defect after the defect area is divided out, so that the detection could be arrived testing requirements for practical application [26-28]. The defective characteristic data comes from the defective image which divided from the detection surface. Despite the data size of divided defect image is much less than the original data collection, the defect image still uses pixel as data units.

### 3. Defect Detection Technologies on the Surface of Magnetic Sheet

#### 3.1. The Template Positioning of Magnetic Sheet and the Creation of Fixed Coordinate System

In this paper, the object which needs to be detected is a magnetic sheet of square piece fillet, which is a kind of permanent magnet material made of sintered NdFeB. The images of magnetic sheet to be detected are obtained via a CCD camera. This magnetic sheet presents gray at natural state, first white-light source is used to illuminate on the magnetic sheet, then the magnetic sheet is shot, which can highlight the differences between the target of images and the background of images for the sake of reducing the difficulty of image processing operations in the next step. Because magnetic sheet has two surfaces, the white-light source should illuminate equably and perpendicularly on the magnetic sheet upper surface when the camera shoot.

**3.1.1. The Template Positioning of Magnetic Sheet:** In order to reduce the data quantity used in operation and improve the running speed of the program, the original image should be segmented before positioning the magnetic sheet image template, and a binary image is generated. In this paper, magnetic sheet image only has target and background, and the two parts could be separated by a threshold value, therefore a single thresholding method is used for disposing image binary segmentation [29, 30].  $T$  represents the gray threshold used in the binary segmentation of image. The target and background could be separated in the input image.  $f(i,j)$  represents the initial image,  $g(i,j)$  represents the divided image. The single thresholding method of magnetic sheet image is expressed as follow.

$$g(i,j) = \begin{cases} 0 & f(i,j) < T \\ 255 & f(i,j) \geq T \end{cases} \quad (1)$$

Obviously, the magnetic sheet which needs to be processed has two surfaces, and image processing of upper surface of magnetic sheet is taken as an example in this paper. The theory of setting gray threshold  $T$  is based on the analysis result of gray histogram of the magnetic sheet image, and the appropriate threshold value  $T$  is set according to the distribution of gray range. Because magnetic sheets in the same kind have the same background, the gray level distribution in original image of only one magnetic sheet is analyzed in this paper. The image before binary segmentation of the upper surface on the magnetic sheet is as shown in Figure 1.

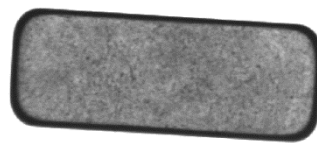


**Figure 1. Upper Surface of Magnetic Sheet before Binary Image Segmentation**

The steps using a single thresholding method for binary segmentation on the original image of the magnetic sheet upper surface are as follows.

step 1: The original image of magnetic sheet is loaded from file which means that LoadImage, the original image of magnetic sheet is the image in Figure 1; step 2: About input image, width nWidth, height nHeight, the size of the line nWidthStep, gray threshold value nThreshold, the array of image data pImageData are set;
---

step 3: The gray threshold value  $n_{Threshold}$  is used for dividing the magnetic sheet image;  
step 4: It is judged whether each regional pixel area after binary segmentation is smaller than the setting minimum area of pixel or not, then the smaller areas are set to 0xff;  
step 5: The magnetic sheet image is saved after binary segmentation which means that SaveImage.

Image of upper surface of magnetic sheet after disposed through single thresholding is as shown in Figure 2.



**Figure 2. Upper Surface of Magnetic Sheet after Binary Image Segmentation**

After upper surface image of magnetic sheet is carried on the binary segmentation through a single thresholding method, the output image will be used as the input image of the template positioning of magnetic sheet image in next step.

Before the PatQuick algorithm is used for carrying on template positioning for the magnetic sheet upper surface image, first the image should be trained to produce a training template, after the training template is saved, the template positioning is matched for the image. Training template image is a magnetic sheet image without defects, the training process is as follows.

step 1: The image that upper surface of standard magnetic sheet after binary segmentation as shown in Figure 2 will be the image source of training template;  
step 2: Training image is gained;  
step 3: Training area and origin point are set;  
step 4: Training parameters are set;  
step 5: Template is trained;  
step 6: Training results are gained;  
step 7: Training results are evaluated;  
step 8: Training template is saved.

PatQuick algorithm is used for confirming all characteristics in image when training image. Characteristic represents contour line between the different areas in image, which means that a series of demarcation points along the contour line. The steps of locating magnetic sheet image are as follows.

step 1: The image that upper surface of standard magnetic sheet after binary segmentation will be the image source of training template;  
step 2: Training template is loaded;  
step 3: Runtime parameters are set;  
step 4: Locating image is gained;  
step 5: PatQuick algorithm is run;  
step 6: Locating result is gained and the coordinate of the image is output after locating.

The image of magnetic sheet upper surface after binary segmentation need to be located and a set of data will be gained, which include the magnetic sheet image's TranslationX, TranslationY and Ration, among this, TranslationX represents the point in image which was found relative to the center x coordinate value of the original training images, TranslationY represents the point in image which was found relative to the center y coordinate value of the original training images,

Ration represents the angle in image which was found relative to the rotation angle of the original training images. The group of data will be set as input data to create magnetic sheet of fixed coordinate system.

**3.1.2. The Creation of Fixed Coordinate System of Magnetic Sheet:** After completing image matching, the root coordinates of the input image is found, it means that the left-handed coordinate system is found, the left-handed coordinate system should be consistent with the collected image pixels before the input image is disposed; and geometric transformation could map the root coordinates to the fixed coordinate system of the template.

These include image translation, scaling and rotation. Image translation means that all points in image are moved according to the setting value in horizontal and vertical. As shown in Figure 3,  $(x_0, y_0)$  is assumed a point in original image and the horizontal translation of image is set as  $t_x$ , the horizontal translation of image is set as  $t_y$ , then the point after translation will be  $(x_1, y_1)$ .

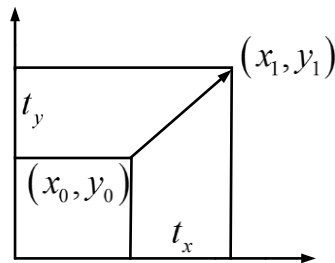


**Figure 3. Schematic Image Translation**

The relation matrix between coordinate  $(x_0, y_0)$  and  $(x_1, y_1)$  is shown as follows.

$$\begin{pmatrix} x_1 \\ y_1 \\ 1 \end{pmatrix} = \begin{pmatrix} 1 & 0 & t_x \\ 0 & 1 & t_y \\ 0 & 0 & 1 \end{pmatrix} \begin{pmatrix} x_0 \\ y_0 \\ 1 \end{pmatrix}$$

The inverse operation is calculated for the above expression, and the inverse transform will be achieved

$$\begin{pmatrix} x_0 \\ y_0 \\ 1 \end{pmatrix} = \begin{pmatrix} 1 & 0 & -t_x \\ 0 & 1 & -t_y \\ 0 & 0 & 1 \end{pmatrix} \begin{pmatrix} x_1 \\ y_1 \\ 1 \end{pmatrix}$$

Means that  $\begin{cases} x_0 = x_1 - t_x \\ y_0 = y_1 - t_y \end{cases}$

If the point in image after translation could not match the corresponding point in the original image, the pixel value is directly set as 0 or 255, and then the translation operation of image is achieved.

The zoom of image is to transform the size of image according to the given ratio, the image after scale changed may not find the corresponding pixels in the original image, so it must be disposed approximately. Usually, the value is set as its closest pixel value directly, and the interpolation algorithm should also be used for calculating the value.

It is assumed that the zoom scaling factor is  $f_x$  at X direction of principal axis in the image, and the zoom scaling factor is  $f_y$  at Y direction of principal axis, and so the transformation matrix from the point  $(x_0, y_0)$  in the original image to the point  $(x_1, y_1)$  in the new image is

$$\begin{pmatrix} x_1 \\ y_1 \\ 1 \end{pmatrix} = \begin{pmatrix} f_x & 0 & 0 \\ 0 & f_y & 0 \\ 0 & 0 & 1 \end{pmatrix} \begin{pmatrix} x_0 \\ y_0 \\ 1 \end{pmatrix}$$

The expression of inverse operation is

$$\begin{pmatrix} x_0 \\ y_0 \\ 1 \end{pmatrix} = \begin{pmatrix} 1/f_x & 0 & 0 \\ 0 & 1/f_y & 0 \\ 0 & 0 & 1 \end{pmatrix} \begin{pmatrix} x_1 \\ y_1 \\ 1 \end{pmatrix},$$

Means that  $\begin{cases} x_0 = x_1/f_x \\ y_0 = y_1/f_y \end{cases}$ .

The rotation of image is generally seen the center in image as original point and then a certain angle is rotated. The size of the image will be changed after rotation. As shown in Figure 4.

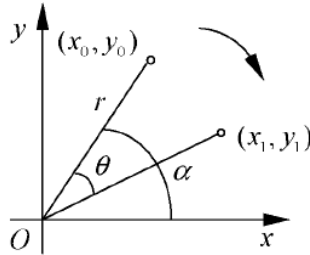


**Figure 4. Schematic Image Rotation**

Before rotation

$$\begin{cases} x_0 = r \cos(\alpha) \\ y_0 = r \sin(\alpha) \end{cases}$$

After rotation, the matrix expression is

$$\begin{pmatrix} x_1 \\ y_1 \\ 1 \end{pmatrix} = \begin{pmatrix} \cos(\theta) & \sin(\theta) & 0 \\ -\sin(\theta) & \cos(\theta) & 0 \\ 0 & 0 & 1 \end{pmatrix} \begin{pmatrix} x_0 \\ y_0 \\ 1 \end{pmatrix},$$

The expression of inverse operation is

$$\begin{pmatrix} x_0 \\ y_0 \\ 1 \end{pmatrix} = \begin{pmatrix} \cos(\theta) & -\sin(\theta) & 0 \\ \sin(\theta) & \cos(\theta) & 0 \\ 0 & 0 & 1 \end{pmatrix} \begin{pmatrix} x_1 \\ y_1 \\ 1 \end{pmatrix}.$$

Setting the centroid coordinates of the target object in input image is set as  $(x_R, y_R)$ , and then the centroid of the target object in input image is.

$$\begin{cases} x_R = \frac{\sum x_i f(x_i, y_i)}{\sum f(x_i, y_i)} \\ y_R = \frac{\sum y_i f(x_i, y_i)}{\sum f(x_i, y_i)} \end{cases} \quad (2)$$

In the expression (2),  $f(x_i, y_i)$  is gray value of target object.

The root coordinate system of input image is  $\{R\}$ , the fixed coordinate system of template is  $\{P\}$ , the mapping from root coordinate system  $\{R\}$  to fixed coordinate system  $\{P\}$  is shown in Figure 5.

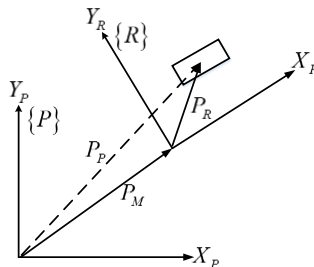


**Figure 5. Coordinate System Transformation from the Root to the Fixed**

So, the expression of mapping transformation from the root coordinate system to the fixed coordinate system is

$$P_P = R_R P_R + P_M \quad (3)$$

In expression (3)

$$P_P = \begin{bmatrix} x_P \\ y_P \end{bmatrix} P_R = \begin{bmatrix} x_R \\ y_R \end{bmatrix}$$

$$R_R = \begin{bmatrix} \cos \theta & -\sin \theta \\ \sin \theta & \cos \theta \end{bmatrix} P_M = \begin{bmatrix} t_x \\ t_y \end{bmatrix}$$

In the upper expression,  $P_P$  represents the coordinate of the target object centroid in input image in the fixed coordinate system  $\{P\}$ ;  $P_R$  represents the coordinate of the target object centroid in input image in the root coordinate system  $\{R\}$ ;  $R_R$  is a rotated mapping matrix sized  $2 \times 2$ ;  $\theta$  is the rotated angle;  $P_M$  is a translation vector sized  $2 \times 1$ . In the expression (3), the homogeneous coordinates could be extracted from the root coordinate system  $\{R\}$  to the fixed coordinate system  $\{P\}$ .

$$\begin{bmatrix} x_P \\ y_P \\ 1 \end{bmatrix} = \begin{bmatrix} \cos \theta & -\sin \theta & t_x \\ \sin \theta & \cos \theta & t_y \\ 0 & 0 & 1 \end{bmatrix} \begin{bmatrix} x_R \\ y_R \\ 1 \end{bmatrix} \quad (4)$$

Substitute the expression (2) of centroid coordinates substituted into the expression (4) of homogeneous coordinate transformation, and will gain

$$\begin{bmatrix} x_P \\ y_P \\ 1 \end{bmatrix} = \frac{1}{\sum f(x_i, y_i)} \begin{bmatrix} \cos \theta & -\sin \theta & t_x \\ \sin \theta & \cos \theta & t_y \\ 0 & 0 & 1 \end{bmatrix} \begin{bmatrix} \sum x_i f(x_i, y_i) \\ \sum y_i f(x_i, y_i) \\ \sum f(x_i, y_i) \end{bmatrix} \quad (5)$$

At present, the position compensation values  $\theta$ ,  $t_x$ ,  $t_y$  could be gained in template matching, the coordinate of the fixed coordinate system  $\{P\}$  could be calculated with the formula (5) in this system, and geometric transformation between the root coordinate system and the fixed coordinate system is realized.

The establishment of fixed coordinate system of magnetic sheet image regards the group of data TranslationX、 TranslationY and Ration output from template positioning as the input data. The fixed steps of the upper surface of the magnetic sheet are as follows.

- step 1: In the program, image in Figure 1 is regarded as the source image.
- step 2: The input data is set. The data of location searching TranslationX、 TranslationY and Ration is regarded as the corresponding input data.
- step 3: The program is run and image after immobilization will be output.

After the magnetic sheet upper surface has fixed, the image as shown in Figure 6, and it will be generated a fixed image as input image in the subsequent processing

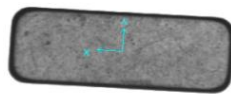


**Figure 6. Fixed upper Surface Image of Magnetic Sheet**

### 3.2. The Extraction of Target Area with the Method of Maximum Entropy

The optimal threshold of image is calculated through the maximum entropy method, in fact, the step means the segmentation threshold which makes the sum of information entropy of the target and information entropy of the background in image biggest is calculated. Setting size of image is  $M \times N$ , gray level is  $L$ . Assumed that there is  $N_i$  pixel which gray level equals to  $i$ , and then the probability of gray level  $P_i$  is

$$P_i = \frac{N_i}{N \times M} \quad (6)$$

The entropy of image target area  $H_f$  and the entropy of image background area  $H_b$  are respectively in expression (7) and (8).

$$H_f = -\sum_{i=1}^T \frac{P_i}{P_t} \log \frac{P_i}{P_t} \quad (7)$$

$$H_b = -\sum_{i=T+1}^L \frac{P_i}{1-P_t} \log \frac{P_i}{1-P_t} \quad (8)$$

In the expression (7) and (8), the expression of  $P_t$  is  $P_t = \sum_{i=1}^T P_i$ .

Finally the best threshold formula is

$$T^* = \operatorname{argmax}[H_f(T) + H_b(T)] \quad (9)$$

Each gray level of image is visited, and the gray level which makes the entropy of the background region and the target region be the maximum is found out, and then the best segmentation threshold  $T^*$  is gained.

The maximum entropy method is used for extracting the magnetic sheet target area, and the operation steps are shown as follows.

step 1: The upper surface of the original magnetic sheet image is input to dispose;  
 step 2: The probability of each grayscale is calculated;  
 step 3: The original Segmentation threshold is set as  $Th$ , the image will be split into two parts by  $Th$ , one is the gray value smaller than  $Th$  and the other is the gray value bigger than  $Th$ ;  
 step 4: The entropy of magnetic sheet background region and entropy of magnetic sheet target region is calculated according to the calculation formula of entropy.  
 step 5: Each gray level of image is visited, and the sum of the entropy of magnetic sheet background region and the entropy of magnetic sheet target region is the biggest gray level is looked for.  
 step 6: The extractive target area according to the magnetic sheet image divided by gray level in step 5 is gained.

The target area of magnetic sheet image divided by maximum entropy method is as shown in Figure 7.



**Figure 7. Target Area of upper Surface of Magnetic Sheet Segmented by Maximum Entropy Method**

### 3.3. The Detection of Knock Edge of Magnetic Sheet

The template positioning of magnetic sheet and the creation of fixed coordinate system have the same purpose for the sake of the knock edge detection of magnetic sheet. The knock edge detection of magnetic sheet is based on image after the creation of fixed coordinate system. Two knock edges need to be detected. One is the edge of straight line and the other is the edge of circular bead. So there are eight edges of straight line and eight edges of circular bead to be detected.

**3.3.1. The Detection of Magnetic Sheet Straight edge:** Figure 7 shows that 16 edges need to be detected on the upper surface of magnetic sheet which include respectively two edges of straight line at upper, lower, right and left, and respectively two edges of circular bead at left-up, left-down, right-up, right-down. For this reason, respectively, the linear fitting method and circle fitting method are used.

The process of fitting a straight line as follows.

step 1: The image shown in Figure 7 is set as the input image in the program;  
 step 2: The best-fitting straight line is put at the line to be searched, and then the length is adjusted;  
 step 3: The number of practical caliper is set, the more caliper, the more accurate;  
 step 4: The search direction of the caliper is set, the direction usually perpendicular to the direction of the best-fitting straight line, it means the angle is 90;  
 step 5: The search length on the direction of caliper is set;  
 step 6: The projected length of caliper is set, it means the search width of caliper;  
 step 7: The edge model is set as single edge, the polarity of edge is determined by the search direction from light to dark or dark to light;  
 step 8: Some boundary points are gained, and the number should be same with the number of caliper;  
 step 9: All boundary points are fit a line with the method of linear fitting, and the abnormal points are excluded.  
 step 10: The distance from each point to the fitting straight line is gained.

The lower outer line of magnetic sheet upper surface after fitted is as shown in Figure 8.

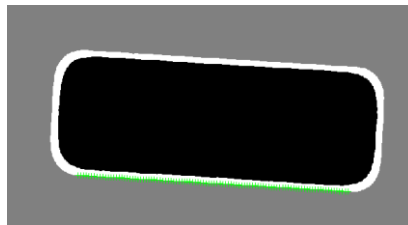


**Figure 8. After Fitting a Straight Line Image**

After the boundary points are found, the points are fitted a straight line. The theory of fitting straight line is based on polynomial fitting of least square method, and the simple linear model is  $y = a_0 + a_1x$  at when  $n = 1$ . The distance from each boundary point to the fitting straight line is calculated, and then compared the distance with the standard distance, a knock edge is predicated if the distance is bigger than the standard distance.

### 3.3.2. The Detection of Magnetic Sheet Fillet Edge: Circle fitting

The equation of circle is

$$(X - m)^2 + (Y - n)^2 = R^2 \quad (10)$$

Here, the residual is set as

$$\xi_i = (X_i - m)^2 + (Y_i - n)^2 - R^2 \quad (11)$$

Residual sum of squares is

$$Q = \sum_{i \in \pi} \xi_i^2 = \sum_{i \in \pi} [(X_i - m)^2 + (Y_i - n)^2 - R^2]^2 \quad (12)$$

In expression (12),  $(m, n)$  represents central coordinate of circle,  $R$  represents radius,  $i \in \pi$ ,  $\pi$  represent the collection of the point on the circle.

According to the theory of least square method

$$\frac{\partial Q}{\partial m} = \frac{\partial Q}{\partial n} = \frac{\partial Q}{\partial R} = 0$$

$$\Rightarrow \begin{cases} \frac{\partial Q}{\partial m} = 2 \sum_{i \in \pi} [(X_i - m)^2 + (Y_i - n)^2 - R^2](-2)(X_i - m) = 0 \\ \frac{\partial Q}{\partial n} = 2 \sum_{i \in \pi} [(X_i - m)^2 + (Y_i - n)^2 - R^2](-2)(Y_i - n) = 0 \\ \frac{\partial Q}{\partial R} = 2 \sum_{i \in \pi} [(X_i - m)^2 + (Y_i - n)^2 - R^2](-2)R = 0 \end{cases}$$

$$\Rightarrow \begin{cases} m^2 - 2\bar{X}m + n^2 - 2\bar{Y}n - R^2 + \bar{X}^2 + \bar{Y}^2 = 0 \\ \bar{X}m^2 - 2\bar{X}^2m + \bar{X}n^2 - 2\bar{X}\bar{Y}n - \bar{X}R^2 + \bar{X}^3 + \bar{X}\bar{Y}^2 = 0(13) \\ \bar{Y}m^2 - 2\bar{Y}^2m + \bar{Y}n^2 - 2\bar{X}\bar{Y}m - \bar{Y}R^2 + \bar{Y}^3 + \bar{X}^2\bar{Y} = 0 \end{cases}$$

The parameters in expression (13) could use the expression below.

$$\bar{X}^A \bar{Y}^B = \sum_{i \in \pi} X_i^A Y_i^B / \sum_{i \in \pi} 1 \quad (14)$$

The parameters  $m^2$ 、 $n^2$ 、 $R^2$  are eliminated in formula(13), and further simplified of the expression is

$$\begin{cases} m = \frac{(\bar{X}^2\bar{X} + \bar{X}\bar{Y}^2 - \bar{X}^3 - \bar{X}\bar{Y}^2)(\bar{Y}^2 - \bar{Y}^2) - (\bar{X}^2\bar{Y} + \bar{Y}\bar{Y}^2 - \bar{X}^2\bar{Y} - \bar{Y}^3)(\bar{X}\bar{Y} - \bar{X}\bar{Y})}{2(\bar{X}^2 - \bar{X}^2)(\bar{Y}^2 - \bar{Y}^2) - 2(\bar{X}\bar{Y} - \bar{X}\bar{Y})^2} \\ n = \frac{(\bar{X}^2\bar{Y} + \bar{Y}\bar{Y}^2 - \bar{Y}^3 - \bar{X}^2\bar{Y})(\bar{X}^2 - \bar{X}^2) - (\bar{X}^2\bar{X} + \bar{X}\bar{Y}^2 - \bar{X}\bar{Y}^2 - \bar{X}^3)(\bar{X}\bar{Y} - \bar{X}\bar{Y})}{2(\bar{X}^2 - \bar{X}^2)(\bar{Y}^2 - \bar{Y}^2) - 2(\bar{X}\bar{Y} - \bar{X}\bar{Y})^2} \\ R = \sqrt{m^2 - 2\bar{X}m + n^2 - 2\bar{Y}n + \bar{X}^2 + \bar{Y}^2} \end{cases} \quad (15)$$

From the formula (15), the form of detecting algorithm is complex, the center and radial of the circle is calculated in the algorithm according to the theory of circle fitting least squares, but each parameter could be calculated by one cycle of boundary point, the time complexity is  $O(n)$ . The more complicated operation of square root is calculated once after the center parameters  $a$ 、 $b$  is calculated, so the operating rate of the algorithm run still fast. The detection principle of the other straight line on the magnetic sheet upper surface is the same with the detection principle mentioned in the preceding part of the lower outer line on the magnetic sheet.

The detection of the eight fillet edges on the magnetic sheet upper surface also need to gain some boundary points with a caliper, and then the boundary points is fitted arc, the coordinates of the circle center and radius is found. The theory is based on circle fitting of the least squares method. The distance from each boundary point to the center of circle is calculated, and the distance is compared with the standard distance, it is determined a knock edge if the distance is bigger than the standard distance. The detection schematic diagram of the right-down fillet at the magnetic sheet upper surface is as shown in Figure 9.



**Figure 9. Detection Schematic Outer Chamfered Surface Right on Diskette**

After 16 sides of magnetic sheet is detected one by one, and then according to the result of detection, the magnetic sheet is detected to own knock edge or not, as long as one knock edge exists in the 16 edges, the result will be determined to have the knock edge. If the knock edge exists, the detection of the magnetic sheet image will end; if the knock edge doesn't exist the detection will enter the next step and pitting and scratches on the magnetic sheet surface should be detected.

## 4. Experimental Result

The surface defects of magnetic sheet to be detected in this paper are divided into two categories: one is knock edge of the rim; the other one is the pocking mark and scratches of surface. The detection process of knock edge is: the detected edge should be taken out, and the edge is fitted, and then the number of boundary points is set, the distance from boundary point to the fitting line will be gained, finally, the distance is compared with the standard distance to judge the edge is knock edge or not. The detection process of the pitting and scratches of surface is: the grayscale distribution of the pitting and the gray distribution of scratches are analyzed, and then grayscale threshold value is set to determine the detection area has pitting and scratches or not.

In this paper, ten groups of experiments for knock edge defect of magnetic sheet have been completed, and each group has been detected 120 magnetic sheets, the knock edge exists in all groups. The result of detection is as shown in Table 1.

**Table 1. Disk Knock the Edge Defect Detection Results**

Group number	Detected number	Observed number	Detection rate (%)
1	120	108	90.0
2	120	109	90.8
3	120	109	90.8
4	120	108	90.0
5	120	107	89.2
6	120	106	88.3
7	120	108	90.0
8	120	107	89.2
9	120	109	90.8
10	120	108	90.0

## 5. Conclusion

In this paper, according to the characteristics of magnetic sheet image background and magnetic sheet image target, the single threshold method is used for the binary segmentation of magnetic sheet image, and then binary segmentation image is obtained; then PatQuick algorithm is used for its template positioned on the magnetic sheet binary segmentation image, good results is gained and the data used in the next step is obtained; the maximum entropy method is used to extract the target area of magnetic sheet image could meet the next requirement of detection knock edge, and then the distance from boundary points to fitting boundary is calculated in order to detect the knock edge of magnetic sheet.

The in-depth study has done in this paper about the magnetic sheet surface defect detection, but in order to improve the detection accuracy, the impact of abnormal point should be considered when fitting the straight line and fillet line by the method of least square.

## ACKNOWLEDGEMENT

This paper is sponsored by the New Century Program for Excellent Talents of the Ministry of Education of China, Liaoning province innovation group project (LT2011005), the Shenyang Ligong University Computer Science and Technology Key Discipline Open Foundation (2012, 2013), Liaoning fourth batch of distinguished professor project (2014) and Liaoning BaiQianWan Talents Program (2014921042).

## Referece

- [1] R. Geng and J. Peng, "On the Flourishing Development of NDT Techniques in China", *Journal of Mechanical Engineering*, no. 49, (2013), pp. 1-7.
- [2] Z. Yuan, "Application and Development of Nondestructive Testing Technology in Mechanical Industry", *Journal of Hubei University for Nationalities (Natural Science Edition)*, no. 31, (2013), pp. 228-231.
- [3] S. Liu and F. Yin, "The Basic Principle and Its New Advances of Image Segmentation Methods Based on Graph Cuts", *ACTA AUTOMATICA SINICA*, no. 38, (2012), pp. 911-922.
- [4] Y. Xie and L. Yang, "Level Set Method of Image Segmentation Based on Adaptive Model", *Computer Engineering and Applications*, no. 47, (2011), pp. 221-224.
- [5] F. Liu, Z. Zhang, N. Wang and J. Shen, "Adaptive Edge Detection Based on Image Region Characteristics", *Application Research of Computer*, no. 29, (2012), pp. 2382-2384.
- [6] M. Wang, Y. Li and X. Quan, "A Survey on Graph Theory Approaches of Image Segmentation", *Computer Applications and Software*, no. 31, (2014), pp. 1-12.
- [7] C. Geng and F. Fang, "Endoscopic Image Segmentation Method Combined Region Growing and Hough Transformation", *Journal of Applied Optics*, no. 35, (2014), pp. 1009-1015.
- [8] S. Xu, J. Han and G. Liu, "Survey of Image Segmentation Methods Based on Markov Random Fields", *Application Research of Computers*, no. 30, (2013), pp. 2576-2582.
- [9] J. Wang, S. Wang and Z. Deng, "Fast Kernel Density Estimator Based Image Thresholding Algorithm for Small Target Images", *ACTA AUTOMATICA SINICA*, no. 38, (2012), pp. 1679-1689.
- [10] J. Long, X. Shen and H. Chen, "Adaptive Minimum Error Thresholding Algorithm", *ACTA AUTOMATICA SINICA*, no. 38, (2012), pp. 1134-1144.
- [11] Y. Zhang and N. Kingsbury, "Improved Bounds for Modified Subband-adaptive Iterative Shrinkage/Thresholding Algorithms", *IEEE Transactions on Image Processing*, no. 29, (2012), pp. 1373-1381.
- [12] B. Wang, G. Zhang, Z. Li and J. Wang, "Wavelet Threshold Denoising Algorithm Based on New Threshold Function", *Journal of Computer Applications*, no. 34, (2014), pp. 1499-1502.
- [13] G. Huang, L. Xu and Y. Pu, "Summary of Research on Image Processing using Fractional Calculus", *Application Research of Computers*, no. 29, (2012), pp. 414-420.
- [14] Y. Du, B. Hong, L. Guo and N. Yang, "Novel Curve Fitting Edge Feature Extraction Algorithm", *Journal of Xidian University*, no. 38, (2011), pp. 164-168.
- [15] Y. Zhao, H. Lin and H. Bao, "Local Progressive Interpolation for Subdivision Surface Fitting", *Journal of Computer Research and Development*, no. 49, (2012), pp. 1699-1707.
- [16] J. Zhang and J. Luo, "A Surface Crack Edge Detection Algorithm Based on Improved Sobel Operator", *Journal of Hefei University of Technology*, no. 34, (2011), pp. 846-847.
- [17] L. Li, G. Ma and X. Du, "Edge Detection in Potential-Field Data by Enhanced Mathematical Morphology Filter", *Pure and Applied Geophysics*, no. 4, (2013), pp. 645-653.
- [18] Y. Zhao and S. Dan, "Study on the Defect Detection Technology Based on Wavelet Analysis and Image Edge Detection", *EN*, no. 6, (2012), pp. 125-132.
- [19] F. Dong, Z. Chen and J. Wang, "A New Level Set Method for Inhomogeneous Image Segmentation", *Image and Vision Computing*, no. 31, (2013), pp. 809-822.
- [20] G. Tan, J. Wu, B. Fan and B. Jiang, "Adaptive Template Filter Method for Image Processing Based on Immune Genetic Algorithm", *Journal of Central South University of Technology*, no. 17, (2010), pp. 1028-1035.
- [21] Y. Yu, J. Zheng and X. Guo, "Weight Fuzzy Threshold Segmentation Algorithm Based On Image Pixel Spatial Information", *Computer Applications and Software*, no. 30, (2013), pp. 274-277.
- [22] F. Ma and T. Xu, "Improved Minimum Intensity Change Corner Extraction Algorithm", *Computer Simulation*, no. 29, (2012), pp. 227-229.
- [23] J. Cao, H. Li, Q. Cai and S. Guo, "Research on Feature Extraction of Image Target", *Computer Simulation*, no. 30, (2013), pp. 409-415.
- [24] H. Pan, A. Wang, Z. Cheng and S. Jin, "Cascade Object Matching by Combining Image Feature and Geometry Feature", *Journal of System Simulation*, no. 24, (2012), pp. 113-117.
- [25] X. Gao, Z. Wang, J. Liu, C. Cui and L. Wang, "Variable Domain Algorithm for Image Segmentation Using Statistical Models Based on Intensity Features", *ACTA OPTICA SINICA*, no. 31, (2011), pp. 198-203.
- [26] J. Luo, T. Dong, D. Song and C. Xiu, "A Review on Surface Defect Detection", *Journal of Frontiers of Computer Science and Technology*, no. 9, (2014), pp. 1041-1048.
- [27] C. Yang, G. Yin, H. Jiang and X. Li, "On Magnetic Tile Surfaces Defect Detection Based on Wavelet Transform", *Computer Applications and Software*, no. 31, (2014), pp. 210-213.
- [28] Z. Zhang, R. Bai, Z. Guo and L. Jiang, "The Feature Selection and Bias Classification of Magnetic Tile Surface Defect", *OPTICAL TECHNIQUE*, no. 40, (2014), pp. 434-439.
- [29] J. Ming, J. Ruan and Y. Yang, "Color Image Binarization Method Based on The Characteristics Library", *Computer Engineering and Design*, no. 34, (2013), pp. 1856-1859.
- [30] G. Zhu, H. Yang, X. Yue, A. Leng and Y. He, "Thresholding Image Segmentation Based on Adaptive Maximum Scatter Difference", *Computer Engineering and Applications*, no. 49, (2013), pp. 188-191.

## Authors



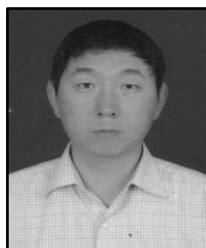
**Wenbo Zhang**, is currently a professor of School of Information Science& Engineering, Shenyang Ligong University, China. He received his Ph.D. in Computer science at Northeastern University, China, in March 2006. He has published over 100 papers in related international conferences and journals. He has served in the editorial board of up to 10 journals, including Chinese Journal of Electronics and Journal of Astronautics. He had been awarded the ICINIS 2011 Best Paper Awards and up to 9 Science and Technology Awards including the National Science and Technology Progress Award and Youth Science and Technology Awards from China Ordnance Society. His current research interests are Ad hoc networks, Sensor Networks, Satellite networks, Embedded systems.



**Rongwei Duan**, is currently a Graduate student of School of Information Science& Engineering, Shenyang Ligong University, China. His current research interests are Ad hoc networks, Sensor Networks, Embedded systems.



**Yongxin Feng**, received the M.S. degree in Computer science from Northeastern University in 2000, and the Ph.D. degree in Computer science from the school of Information and Engineering, Northeastern University 2003. She is currently a professor in Shenyang Ligong University. She has published over 60 papers in related international conferences and journals. He had been awarded the ICINIS 2011 Best Paper Awards and up to 15 Science and Technology Awards including the National Science and Technology Progress Award and Youth Science and Technology Awards from China Ordnance Society. Her research interests are in the areas of Network Management, Wireless Sensor Network, Multimedia Communication and Information Systems.



**Deyu Zhang**, is currently a professor of Communication and network Institute, Shenyang Ligong University, China. He received his Ph.D. in Computer application technology at Nanjing University of Science & Technology, China, in July 2005. He has published over 50 papers in related international conferences and journals. He has served in the editorial board of up to 5 journals, including Journal of Fire Control & Command Control *etc.* He had been awarded up to 15 Science and Technology Awards including the National Science and Technology Progress Award and Youth Science and Technology Awards from China Ordnance Society. His current research interests are System monitoring, Wireless networks, Sensor Networks, Embedded systems.

